Bayesian Inference for Animal Space Use and Other Movement Metrics

Devin S. JOHNSON, Josh M. LONDON, and Carey E. KUHN

The analysis of animal movement and resource use has become a standard tool in the study of animal ecology. Telemetry devices have become quite sophisticated in terms of overall size and data collecting capacity. Statistical methods to analyze movement have responded, becoming ever more complex, often relying on state-space modeling. Estimation of movement metrics such as utilization distributions have not followed suit, relying primarily on kernel density estimation. Here we consider a method for making inference about space use that is free of all of the major problems associated with kernel density estimation of utilization distributions such as autocorrelation, irregular time gaps, and error in observed locations. Our proposed method is based on a data augmentation approach that defines use as a summary of the complete path of the animal which is only partially observed. We use a sample from the posterior distribution of the complete path to construct a posterior sample for the metric of interest. Three basic importance sampling based methods for sampling from the posterior distribution of the path are proposed and compared. We demonstrate the augmentation approach by estimating a spatial map of diving intensity for female northern fur seals in the Pribilof Islands, Alaska.

Key Words: Animal movement; Correlated random walk; Movement metric; Posterior distribution; State-space model; Utilization distribution.

1. INTRODUCTION

The analysis of animal movement via individual telemetry devices has become ubiquitous in the field of ecology. Telemetry devices continue to become smaller yet provide an ever increasing quantity of data. Because of this increase in use, statistical analysis of animal movement has subsequently become more complex often relying on state-space modeling methods (see Patterson et al. 2008, for review). State-space models (SSM) can handle several problems that plague telemetry data such as location error (Anderson-Sprecher

Devin S. Johnson (✉), Josh M. London, and Carey E. Kuhn are researchers at the National Marine Mammal Laboratory, Alaska Fisheries Science Center, National Marine Fisheries Service, NOAA, 7600 Sand Point Way NE, Seattle, WA 98115, USA (E-mail: *devin.johnson@noaa.gov*).

Journal of Agricultural, Biological, and Environmental Statistics, Volume 16, Number 3, Pages 357–370
DOI: 10.1007/s13253-011-0056-8

and Ledolter 1991) and changes in animal behavior (Jonsen, Myers, and James 2007; Morales et al. 2004; Johnson et al. 2008; Gurarie, Andrews, and Laidre 2009). SSMs are typically used to estimate parameters of an individual movement model that forms the basis of the "state" component of an SSM. Secondarily, they may be used to estimate locations for various desired times. These desired times are often at a scale fine enough to construct an estimated path (e.g., Johnson et al. 2008). The SSM also provides error estimates for these predictions. Our goal is to illustrate that, while SSMs are valuable tools for animal movement modeling, there is information contained in the associated predictive distributions that is rarely utilized for making inference on movement related quantities of interest.

Most telemetry studies have progressed beyond plotting locations on a map. Just like a probability distribution is described with summaries such as the mean and variance, the usual procedure for telemetry studies is to describe animal locations with a summary such as distance traveled per day. This summary represents a measurement, analogous to weight or length, obtained from the animal. We use the term *movement metric* for these summaries. Patterson et al. (2008) use the term metric to describe a calculation based on the observed locations. Here we used it to describe a summary of the true path of the animal.

One of the most popular classes of metric are those involving animal use of space or habitat. One of the primary reasons for employing telemetry devices in ecological studies is to determine where in a physical landscape an animal spends time or performs certain behaviors. Of the space use metrics, utilization distributions (Van Winkle 1975) are ubiquitous. Essentially, utilization distributions are two-dimensional probability density surfaces for animal locations. The interpretation of this density is a measure of "time spent" in certain spatial regions.

The kernel density method (Worton 1989) has been the predominant method for utilization distribution inference. In its most basic version the kernel method uses a two-dimensional kernel density estimator to estimate a nonparametric density for observed locations. Kernel methods have some drawbacks with respect to telemetry data. First, telemetry data can be highly autocorrelated, which is a violation of kernel density estimator assumptions. Whether or not this actually presents problems in practice, however, is not clear (Fieberg 2007a; Otis and White 1999). Second, all points are not equally informative. Locations often occur clustered in time by design or by chance. Various weighting methods have been proposed to counteract this problem (Fieberg 2007b; Katajisto and Moilanen 2006). Next, there is a bandwidth parameter that must be chosen which can affect results (Fieberg 2007a; Blundell, Maier, and Debevec 2001; Otis and White 1999). There have been several proposed methods for selecting this parameter (see Horne and Garton 2006; Fieberg 2007a). Finally, a complication arises when trying to estimate a utilization distribution for events that have no direct measurement of location. Modern telemetry devices often have auxiliary information that may be out of temporal alignment with the location data. For example, marine mammal telemetry often incorporates diving information. There might be evident dive events that have no associated location (see Section 3 for example). As another example, consider sections of time for which there is a time gap in the location record. Horne et al. (2007) propose a Brownian bridge method that accounts for unknown use between locations by using a kernel that links pairs of locations.

In order to overcome all of the problems previously mentioned, we take a conceptually different approach to movement metric inference. Herein, we would like to focus on the estimation of space use metrics. Although the method presented here is more general, we feel our proposed method will have the biggest impact on how space use is considered. We view space use metrics as a summary of the true, but unknown, path of the animal(s). This differs from the kernel density approach that uses the intensity function of spatial point process to describe the distribution of animal locations. To accomplish this we make use of a Bayesian approach and the posterior distribution of the complete animal track. The philosophy behind this approach is to use posterior draws of the complete track from which the metric can be directly calculated giving a sample from the metric posterior distribution.

The remainder of the paper is organized as follows. In the next section we introduce a method for making Bayesian inference for movement metrics. Although state-space models are not inherently Bayesian, the benefits of Bayesian inference in the analysis of animal telemetry data are numerous. In Section 3 we present examples of estimating spatial diving intensity of northern fur seals (*Callorhinus ursinus*). We also investigated two other metrics, path sinuosity and speed along the entire trip. In the final section we provide some discussion and possible extensions to the method.

2. METHODS

In this section, we present a method for Bayesian inference for movement metrics from state-space models (SSM) for individual animal movement. Many other papers have focused on the use of Markov Chain Monte Carlo (MCMC) simulation to make Bayesian inference for movement model parameters, e.g., Jonsen, Myers, and Flemming (2003), Jonsen, Flemming, and Myers (2005), Jonsen, Myers, and James (2007). MCMC inference for movement models can be a time-consuming process, even for a single animal. Satellite telemetry devices are becoming relatively inexpensive so that they are regularly deployed on tens or hundreds of animals for a single research project.

In presenting our method we have two main goals: (i) to illustrate posterior predictive inference obtainable from SSM output, as well as (ii) to make these methods practical for modern, large-scale, satellite tag deployment projects. To this end we employ an importance sampling approach based on the posterior mode of the movement model parameters. While the computations necessary for sampling from the track posterior are similar to those required for an MCMC run, by using a two-step importance sampling approach we can explore different model fits via optimization before embarking on a time-consuming sampling run. This can be beneficial if there are a large number of animals possibly requiring different models (e.g., covariates).

2.1. MOVEMENT MODELS AND METRICS

Our method is based on the continuous-time correlated random walk (CTCRW) model of Johnson et al. (2008). Gurarie, Andrews, and Laidre (2009) provide a similar continuous-time model based on distance and turning angles. The general CTCRW model is based on modeling the velocity $\boldsymbol{v}(t)$ of the animal at any time t in $(0, T]$ with

an Ornstein–Uhlenbeck (continuous-time AR(1)) process. The resulting location at time t is given by $\boldsymbol{\mu}(t) = \boldsymbol{\mu}(0) + \int_0^t \boldsymbol{v}(u)\,du$. The benefit of this model is that the location of the animal is defined for any particular time of interest and the variability of the location process scales with different time intervals as well. Times of interest might include regular intervals or times where specific events are recorded for the animal (for examples see section *Application: Northern Fur Seal Movement*). Although we use the CTCRW model herein, the Bayesian method we are presenting can be applied to any movement model that can be placed into the form of a SSM (see Equation (2.1)).

Johnson et al. (2008) illustrate that the CTCRW model can be formed into a Gaussian SSM. The SSM form of the CTCRW is given by two equations, the observation equation and the state equation. Assuming movement in d-dimensional space, these equations are:

$$\mathbf{Y}_i = \mathbf{Z}_i\boldsymbol{\alpha}_i + \boldsymbol{\varepsilon}_i \quad \text{and} \quad \boldsymbol{\alpha}_{i+1} = \mathbf{T}_i\boldsymbol{\alpha}_i + \boldsymbol{\eta}_i; \quad i = 1, \ldots, N, \tag{2.1}$$

where $\mathbf{Y}_i$ is the $d \times 1$ observable location of the animal at time t_i, $\boldsymbol{\alpha}_i = (\boldsymbol{\mu}(t_i), \boldsymbol{v}(t_i))'$ is the $2d \times 1$ current state vector, $\mathbf{T}_i$ and $\mathbf{Z}_i$ are $2d \times 2d$ and $d \times 2d$ transformation matrices, $\boldsymbol{\varepsilon}_i$ are serially independent $N(\mathbf{0}, \mathbf{H}_i)$ errors, and $\boldsymbol{\eta}_i$ are serially independent $N(\mathbf{0}, \mathbf{Q}_i)$ errors. In addition, $\boldsymbol{\varepsilon}_i$ and $\boldsymbol{\eta}_i$ are independent. The initial value, $\boldsymbol{\alpha}_1$, is assumed to be known or distributed $N(\boldsymbol{\phi}_1, \mathbf{Q}_1)$. For notational simplicity we have omitted the fact that $\mathbf{H}_i$, $\mathbf{T}_i$, and $\mathbf{Q}_i$ depend on a vector, say $\boldsymbol{\theta}$, of movement parameters as well as the time difference $\Delta_i = t_{i+1} - t_i$. See Johnson et al. (2008) for CTCRW details of matrix entries. For some number, say $n \leq N$, of the t_i we are able to actually observe $\mathbf{Y}_i = \mathbf{y}_i$, these representing the collected location data.

Now we define a movement metric in a more formal way. A general movement metric is given by $\mathbf{m} = h(\boldsymbol{\alpha}_1, \ldots, \boldsymbol{\alpha}_N)$, where the subscript is associated with the set of times $\mathcal{T} = (t_1, \ldots, t_N)$ and $h(\cdot)$ is a vector-valued function that summarizes the states of the animal in some meaningful way. For example, $\mathcal{T}$ might include times of observed locations augmented with hourly times and $h(\cdot)$ might represent the piecewise distance between hourly locations. This would give a measure of total distance traveled.

2.2. POSTERIOR INFERENCE

Due to the fact that not all (or any) states $\boldsymbol{\alpha}_i$ are known, it is necessary to estimate $\mathbf{m}$ in some fashion. Here we propose a method for Bayesian inference of the unknown metric $\mathbf{m}$ via the posterior distribution of the unknown states which are used to calculate $\mathbf{m}$. The posterior distribution is the conditional distribution of the states given the observed locations (and possibly other movement related covariates). We denote the posterior distribution of the states as $[\boldsymbol{\alpha}|\mathbf{y}]$ where $\boldsymbol{\alpha} = (\boldsymbol{\alpha}_1', \ldots, \boldsymbol{\alpha}_N')'$ and $\mathbf{y} = (\mathbf{y}_1', \ldots, \mathbf{y}_n')'$ is the vector of all observed locations. We use $[\cdot|\cdot]$ to generically represent conditional distributions.

In order to characterize $[\mathbf{m}|\mathbf{y}]$ we often need to calculate expectations of the form

$$\int f(\mathbf{m})[\mathbf{m}|\mathbf{y}]\,d\mathbf{m} = \int f\{h(\boldsymbol{\alpha})\}[\boldsymbol{\alpha}|\mathbf{y}]\,d\boldsymbol{\alpha}. \tag{2.2}$$

For example, we might want to use the posterior mean $\hat{\mathbf{m}} = E[\mathbf{m}]$ as the point estimate of $\mathbf{m}$ (i.e., $f(x) = x$). Unfortunately, the integral is intractable and cannot be performed

analytically. We, therefore, propose the Monte Carlo approximation

$$f(\mathbf{m})[\mathbf{m}|\mathbf{y}]\,d\mathbf{m} \approx J^{-1}\sum_{j=1}^{J} f\left\{h\left(\boldsymbol{\alpha}^{(j)}\right)\right\} \tag{2.3}$$

to compute the integrals, where $\boldsymbol{\alpha}^{(j)}$, $j = 1, \ldots, J$, represents a sample from $[\boldsymbol{\alpha}|\mathbf{y}]$.

Now, we focus on drawing a value $\boldsymbol{\alpha}^{(j)}$ from $[\boldsymbol{\alpha}|\mathbf{y}]$. First, note that

$$[\boldsymbol{\alpha}|\mathbf{y}] = \int [\boldsymbol{\alpha}|\boldsymbol{\theta}, \mathbf{y}][\boldsymbol{\theta}|\mathbf{y}]\,d\boldsymbol{\theta}, \tag{2.4}$$

where the reader will recall that $\boldsymbol{\theta}$ is the vector of movement model parameters. Therefore, we can draw a value from $[\boldsymbol{\alpha}|\mathbf{y}]$ by first drawing $\boldsymbol{\theta}$ from $[\boldsymbol{\theta}|\mathbf{y}]$ and then drawing $\boldsymbol{\alpha}$ from $[\boldsymbol{\alpha}|\boldsymbol{\theta}, \mathbf{y}]$. This illustrates that uncertainty in the parameter values is propagated through to the uncertainty in the true state values.

The following three procedures describe methods for approximating $[\boldsymbol{\theta}|\mathbf{y}]$ with a discrete distribution $[\boldsymbol{\theta}|\mathbf{w}]$, where $\mathbf{w} = (w_1, \ldots, w_M)'$ is a vector of probabilities. They begin as follows. First, obtain the posterior mode $\tilde{\boldsymbol{\theta}}$ by maximizing the posterior distribution of the movement model parameters:

$$[\boldsymbol{\theta}|\mathbf{y}] \propto [\mathbf{y}|\boldsymbol{\theta}][\boldsymbol{\theta}], \tag{2.5}$$

where $[\mathbf{y}|\boldsymbol{\theta}]$ is the likelihood of the parameters and $[\boldsymbol{\theta}]$ is the prior distribution of the parameters. Along with $\tilde{\boldsymbol{\theta}}$, one usually can also obtain the Hessian matrix $\tilde{\boldsymbol{\Sigma}}$ of the log-posterior density. The Kalman filter facilitates fast likelihood evaluations (see Durbin and Koopman 2001, Chapter 7), so the optimization proceeds quickly. Next, we can proceed in one of three ways.

The first method is the most simple and for many applications may give acceptable results; simply use the posterior mode $\tilde{\boldsymbol{\theta}}$ with probability 1. If the majority of metric uncertainties are due to location uncertainty along the path, then this method might prove to be adequate and is faster than the following two methods.

The second method is a variant of the Sample-Importance-Resample (SIR) algorithm (Givens and Hoeting 2005). Draw $\boldsymbol{\theta}^{(1)}, \ldots, \boldsymbol{\theta}^{(M)}$ from $[\boldsymbol{\theta}|\tilde{\boldsymbol{\theta}}, \tilde{\boldsymbol{\Sigma}}]$. This could be some variant of a multivariate normal or t distribution with mean $\tilde{\boldsymbol{\theta}}$ and scale matrix $-\tilde{\boldsymbol{\Sigma}}^{-1}$. For each $\boldsymbol{\theta}^{(j)}$ calculate the importance weight

$$w_j \propto \frac{[\boldsymbol{\theta}^{(j)}|\mathbf{y}]}{[\boldsymbol{\theta}^{(j)}|\tilde{\boldsymbol{\theta}}, \tilde{\boldsymbol{\Sigma}}]}. \tag{2.6}$$

This can be a very efficient approximation if $[\boldsymbol{\theta}|\tilde{\boldsymbol{\theta}}, \tilde{\boldsymbol{\Sigma}}]$ is close to the target density. If, however, it is not close (e.g., tails of the proposal are too light), then importance sampling can produce values with weight that is too heavy. See Givens and Hoeting (2005) for illustration.

The third approach resides between methods 1 and 2 in terms of its black-box nature. It is inspired by the deterministic Integrated Nested Laplace Approximations (INLA) of Rue, Martino, and Chopin (2009) for Gaussian Markov random fields. This approach is summarized as follows.

(1) Form the eigen-decomposition of the covariance matrix $-\tilde{\boldsymbol{\Sigma}}^{-1} = \mathbf{V}\boldsymbol{\Lambda}\mathbf{V}'$.

(2) Explore the principle axes of $[\boldsymbol{\theta}|\mathbf{y}]$ via the parameterization $\boldsymbol{\theta}^{(j)} = \tilde{\boldsymbol{\theta}} + \mathbf{V}\boldsymbol{\Lambda}^{1/2}\mathbf{z}$, where $\mathbf{z}$ is successively incremented from $\mathbf{0}$ one entry at a time by step length, say δ_z, until $\log[\tilde{\boldsymbol{\theta}}|\mathbf{y}] - \log[\boldsymbol{\theta}^{(j)}|\mathbf{y}] > \delta_\pi$.

(3) Repeat by successively incrementing each element of $\mathbf{z}$ by $-\delta_z$.

(4) Finally, form a grid with every combination of the $\boldsymbol{\theta}^{(j)}$ entries saved in the previous two steps and retain with the same δ_π criterion.

(5) Form weights $w_j \propto [\boldsymbol{\theta}^{(j)}|\mathbf{y}]$

The main benefit of the deterministic INLA approach is that it avoids having to select a proposal distribution. The drawbacks of this approach, however, are the unknown number of likelihood evaluations and the potential coarseness in high density areas. As the number of parameters becomes large, this method quickly succumbs to the curse of dimensionality.

After choosing one of the methods to construct the finite approximation $[\boldsymbol{\theta}|\mathbf{w}] \approx [\boldsymbol{\theta}|\mathbf{y}]$, one moves to the final step in drawing $\boldsymbol{\alpha}$ for Equation (2.3). The last step is accomplished using the simulation method of Durbin and Koopman (2002) to draw a value from $[\boldsymbol{\alpha}|\boldsymbol{\theta}, \mathbf{y}]$. A quick summary of this step is as follows:

(1) Draw $\boldsymbol{\theta}^+$ with probability distribution $[\boldsymbol{\theta}|\mathbf{w}]$.

(2) Calculate $\hat{\boldsymbol{\alpha}}_i = E[\boldsymbol{\alpha}_i|\boldsymbol{\theta}^+, \mathbf{y}]$ for times $t_i \in \mathcal{T}$ using the Kalman Filter followed by the Kalman Smoother (together denoted KFS) recursions (Durbin and Koopman 2001, p. 71).

(3) Using the state equation (2.1), the selected $\boldsymbol{\theta}^+$, and the initial distribution $[\boldsymbol{\alpha}_1|\boldsymbol{\theta}^+]$, simulate new states $\boldsymbol{\alpha}_i^+$ from $[\boldsymbol{\alpha}_i|\boldsymbol{\theta}^+]$.

(4) For every time that a location was observed simulate a new location $\mathbf{y}_i^+$ from the observation equation in (2.1) using the corresponding $\boldsymbol{\alpha}_i^+$ from step 3.

(5) Calculate $\hat{\boldsymbol{\alpha}}_i^+$ as in step 2, except use the simulated observations $\mathbf{y}_1^+, \ldots, \mathbf{y}_n^+$ instead of the actual observations.

(6) After concatenating the various state vectors together, $\boldsymbol{\alpha}^{(j)} = \hat{\boldsymbol{\alpha}} + \{\boldsymbol{\alpha}^+ - \hat{\boldsymbol{\alpha}}^+\}$ is a draw from the joint distribution $[\boldsymbol{\alpha}|\boldsymbol{\theta}^+, \mathbf{y}]$.

The standard KFS will give us the distribution $[\boldsymbol{\alpha}_i|\boldsymbol{\theta}^+, \mathbf{y}]$ for any one t_i, but it does not give the covariances for the joint distribution $[\boldsymbol{\alpha}|\boldsymbol{\theta}^+, \mathbf{y}]$. The KFS can be rearranged to give the covariances as well, but *all* pairwise covariances would need to be calculated: a very computationally intensive augmentation to the standard KFS compared to the presented simulation method.

3. APPLICATION: NORTHERN FUR SEAL MOVEMENT

3.1. DATA

To illustrate the utility of the proposed method we analyzed movement data from foraging northern fur seals near the Pribilof Islands, Alaska. Thirteen adult female northern fur seals were instrumented at rookeries on St. Paul Island, AK (57.2°N, 170.3°W) during September and October 2007. Females observed nursing or calling for a pup were captured and equipped with a satellite instrument (Mk10-AF by Wildlife Computers) with an Argos transmitter and time-depth recorder. See Kuhn et al. (2009b) for further deployment details.

The Argos transmitted locations are assigned to on of six location quality classes. From highest quality to least, these are 3, 2, 1, 0, A, B, and Z. Class Z locations have an extremely large error radius and were not used in this study. Classes 0–3 have well documented radii (>1500, 500–1500, 250–500, and <250 meters, respectively) corresponding to the standard deviation of the measurement error (CLS 2008). Classes A and B do not have a published error radii.

3.2. METRICS

We examined three basic metrics which are often used in pinniped telemetry studies, sinuosity, speed, and space use. Sinuosity equals the total distance traveled divided by an appropriate straight-line distance. This gives a measure of how "directed" a path the animal traveled. In this example, we used the maximum displacement from the rookery for our straight-line distance. Because northern fur seals are central place foragers (animal returns to the place of trip origin), the sinuosity value has a lower bound of two. We examined this metric because it results in a scaler value for each animal, thus making comparisons between the $\boldsymbol{\theta}$ sample methods straightforward. The speed metric illustrates inference for a time-indexed metric. Finally, as an example of space use inference, we examined a spatial measure of foraging using dive intensity (dives per unit time) on a 10 km grid over the Bering Sea continental shelf.

We chose diving intensity as a our space use metric because "time spent" in a certain location (as is the interpretation of a traditional kernel based utilization distributions) is not always that informative for northern fur seals. Animals tend to rest in long bouts during the daytime, meaning that hot spots we would detect in the map would most likely be resting locations. This is an example where traditional kernel methods would not work due to the fact that times of dive events rarely have an associated observed location. Thus, kernel methods would involve some subjective interpolation of locations and the uncertainty in this would not be propagated to the final inference. In some instances the interpolations may prove to be a very poor approximation to the missing locations.

In order to calculate dive intensity we first processed (IKNOS-DIVE, IKNOS toolbox for MATLAB, Y. Tremblay's unpublished paper) the 5-second depth measurements from the Mk10-AF time-depth recorder into *dives* that have an associated start time, maximum depth, number of "wiggles," and duration. A dive was defined by a minimum depth of

four meters and a minimum duration of 20 seconds. The wiggles are the number of times the animal changed vertical direction. A large number of wiggles is indicative of pursuit of prey during a dive (Kuhn et al. 2009a). We then classified *foraging* dives to be those >10 m and having >5 wiggles. While this designation is somewhat subjective, we feel these conditions provided a conservative assessment of foraging (i.e., some foraging dives are likely to be discarded, but, in our opinion, the chosen dives retained a high likelihood of being conducted in the pursuit of prey). For each animal and each cell of the spatial grid, diving intensity is defined as the number of foraging dives initiated in that cell, divided by the time spent in that cell.

3.3. ESTIMATION

Before simulation a basic CTCRW model was fitted to the data to obtain the posterior mode, $\tilde{\boldsymbol{\theta}}$, of the movement parameters for each animal. The parameters include $\log \tau_0$, $\log \tau_A$, $\log \tau_B$, $\log \sigma$, and $\log \beta$. The τ parameters correspond to the measurement errors for location classes 0, A, and B. For location classes 3, 2, and 1, we used the largest value of the published Argos error radii, 250, 500, and 1500 m, respectively (CLS 2008). A 1500-m lower bound was set for the remaining τ. The parameters σ and β are the CTCRW movement parameters corresponding to variance and autocorrelation of the velocity. Flat priors were used for all parameters; thus, the posterior mode is the maximum likelihood estimate. Finally, for each female we assumed $\boldsymbol{\alpha}_1 = (\boldsymbol{\mu}_1, \mathbf{0})'$ was known, where $\boldsymbol{\mu}_1$ is the release location and the velocity process $\boldsymbol{v}(t)$ was independent between the two spatial coordinates.

Following the initial model fitting, the measurement error shock diagnostic of de Jong and Penzer (1998) was used to eliminate observations in gross error. This is essentially a goodness-of-fit test based on the predictive distribution of the observation in question given all other observations. The model was then refitted to obtain $\tilde{\boldsymbol{\theta}}$ and $\tilde{\boldsymbol{\Sigma}}$. We used the R statistical software (R Development Core Team 2010) to perform all CTCRW model fitting and simulation. The R package `crawl` (v. 1.1–1) was updated to include the sampling methodology presented herein. Both are available from CRAN (*http://cran.r-project.org/*).

To implement the procedure, observed data for each animal was augmented with uniform times on a 15-minute interval and the diving times for each animal. These augmented times and the observed location times form the metric set of times $\mathcal{T}$. For each sampling iteration, $\boldsymbol{\alpha}_i$ was drawn for every t_i in $\mathcal{T}$. In each grid cell the number of dive locations was tallied as well as the number of locations on the 15-minute time scale. Dive intensity was calculated as the ratio of these two counts. Sinuosity was calculated via

$$\frac{\sum_i \|\boldsymbol{\mu}(t_{i+1}) - \boldsymbol{\mu}(t_i)\|}{\max_i \|\boldsymbol{\mu}(t_1) - \boldsymbol{\mu}(t_i)\|},$$

where here the t_i come from the augmented 15-minute interval set and $\|\cdot\|$ represents $\mathbb{R}^2$ Euclidean distance.

In order to assess if there might be sizable differences between the $\boldsymbol{\theta}$ sample methods, we created three $[\boldsymbol{\theta}|\mathbf{w}]$ corresponding to the three presented methods. For the importance sampling method (method 2), a multivariate normal proposal distribution was used (truncated to the lower bounds of the free τ parameters) with a sample size of 3,125. This is the

number of posterior evaluations the INLA method will need using $\delta_z = 1$ and $\delta_\pi = 2.5$ if the posterior is normally distributed (5 points on each axis raised to the $\dim(\boldsymbol{\theta}) = 5$ power). We chose $\delta_z = 1$ and $\delta_\pi = 2.5$ as suggested by Rue, Martino, and Chopin (2009). Using these settings, the number of points retained with the INLA approximation under posterior normality would be 333.

While there are many other choices for the options in approximation methods 2 and 3, we felt like these represented sensible default choices. We attempted to match computational effort as measured both by likelihood evaluations as well as researcher time. Therefore, we only used the default choices of each method to avoid biasing effort by spending more time "hand-tuning" one approximation over the other. While not especially important in this small example, hand-tuning the method for individual animals can prove challenging and time-consuming for studies with hundreds of animals. Finally, following construction of each $[\boldsymbol{\theta}|\mathbf{w}]$ we sampled 5000 draws from $[\boldsymbol{\alpha}|\mathbf{y}]$ for metric inference.

3.4. RESULTS

The maximum number of posterior evaluations for the INLA method was 3,125, exactly equal to the expected number under normality. The minimum was 18 for Animal 3. The number of retained points ranged from 11 to 333 giving retention rates of 11–40% (approximately 10% is expected under normality). From these results we can infer that the posteriors are not exceptionally heavy-tailed. The posterior densities dropped fast enough so that there were only 2–4 points along each axis, similarly to a normal distribution. The efficiency of the SIR weights, however, tells that the posteriors were not all normally shaped. The SIR efficiency is a measure of how close the proposal distribution matches the posterior distribution. An estimator of SIR efficiency is given by $1/(1 + CV^2)$, where CV is the sample coefficient of variation for the weights $\mathbf{w}$ (Givens and Hoeting 2005, p. 164). In this analysis the SIR efficiency ranged from 0.06% (Animal 2) to 85% (Animal 11) with a mean of 44%. Thus, on average, the SIR approximation of $[\boldsymbol{\theta}|\mathbf{w}]$ was equivalent to an approximation based on 1,370 i.i.d. draws from $[\boldsymbol{\theta}|\mathbf{y}]$ and ranged from 2 to 2,668 over the 13 animals. Thus, while the posteriors are light-tailed in this example, the truncated normal is not necessarily a good approximation for all animals, notably Animal 2.

Sample tracks from the INLA method for two different individuals are illustrated in Figure 1. One can see two different types of movement in these animals. The northerly animal (Animal 9) is a mid-shelf forager and travels very purposely on its route. The route of the easterly animal (Animal 11) is a near-shelf forager and has more uncertainty in location in the observation gaps due to its more meandering mode of travel. It is necessary where estimating movement metrics to account for this disparity in uncertainty.

Figure 2 illustrates the estimated sinuosity metric for all 13 animals using each of the three $[\boldsymbol{\theta}|\mathbf{w}]$ approximation methods. As expected, the mode-only method produced the smallest intervals as $\boldsymbol{\theta}$ uncertainty is not taken into account. For the most part, the SIR method had the largest estimates of sinuosity uncertainty, while the INLA method fell in between the other two. The exception was Animal 2. The SIR method was extremely inefficient for this animal. For simplicity, we will present the remaining metric results using

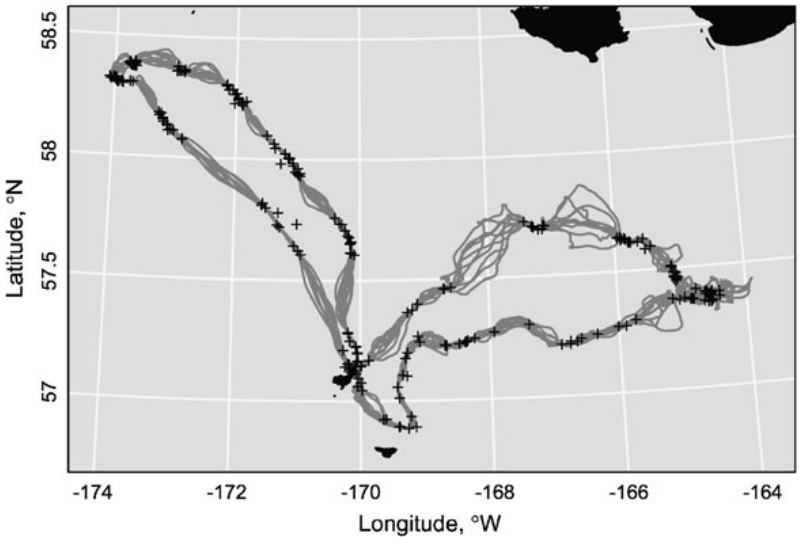

Figure 1. Sample tracks for two different northern fur seals. The northerly paths are from a mid-shelf forager (Animal 9) with more purposeful travel. The easterly paths are from an individual (Animal 11) that travels in a more meandering path. For each Animal 10, posterior sample paths are shown. The black crosses are the observed Argos locations.

just the INLA approximation. The results of the comparison between $[\boldsymbol{\theta}|\mathbf{w}]$ methods were analogous for the other metrics.

The speed metric is shown in Figure 3. Plot (a) shows the mean and 95% credible interval for a the speed of Animal 9 on a 15-minute time scale. One can see the generally diurnal cycle of resting and traveling/foraging. Northern fur seals are known to forage at night with the vertical migration of prey (Goebel 1998). One can also see a general trend of decreasing speed as the animal leaves the rookery and increasing speed as the animal

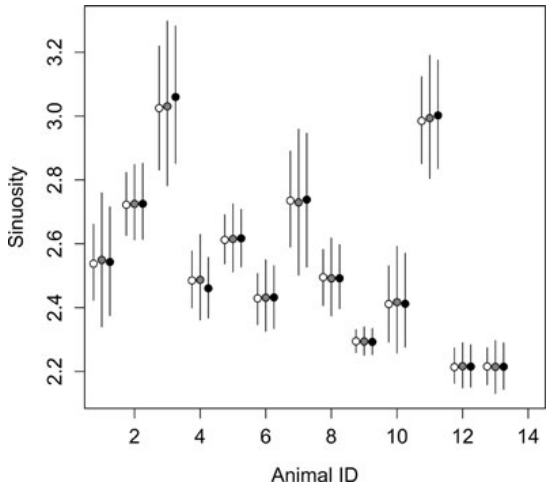

Figure 2. Posterior sinuosity estimates. Points and error bars represent posterior means and 95% credible (HPD) intervals for the posterior-mode-only approximation (white), traditional sample-importance-resample (SIR; gray), and the INLA approximation (black).

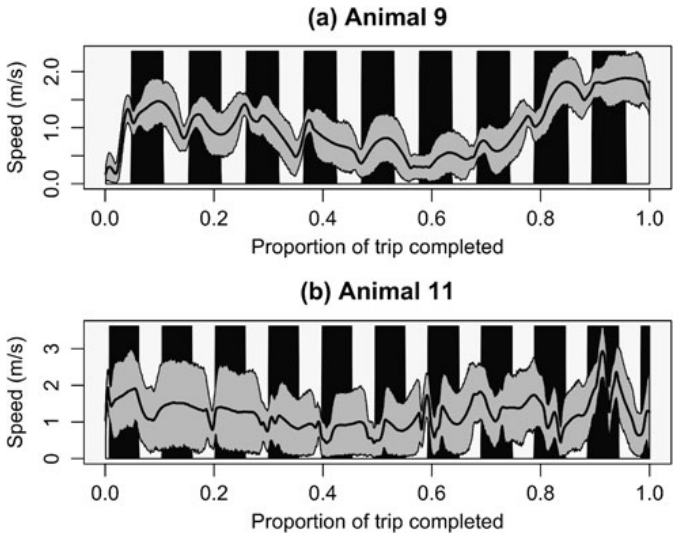

Figure 3. Posterior speed (m/s) estimates. Plot (a) illustrates the posterior distribution of speed for Animal 9. The gray area represents the 95% credible (HPD) interval and the black line represents the posterior mean speed at each time. Black bars represent night hours. Plot (b) illustrates the posterior summary for Animal 11.

returns to the rookery to feed her pup. This general pattern is also evident with Animal 11 (Figure 3 plot (b)). However, the diurnal pattern is not as evident and variation seems more erratic. Combining the information obtained from sinuosity and speed metrics it appears that Animal 9 is using previous knowledge to visit a known foraging path, while Animal 11 seems to be in a more exploratory mode of foraging.

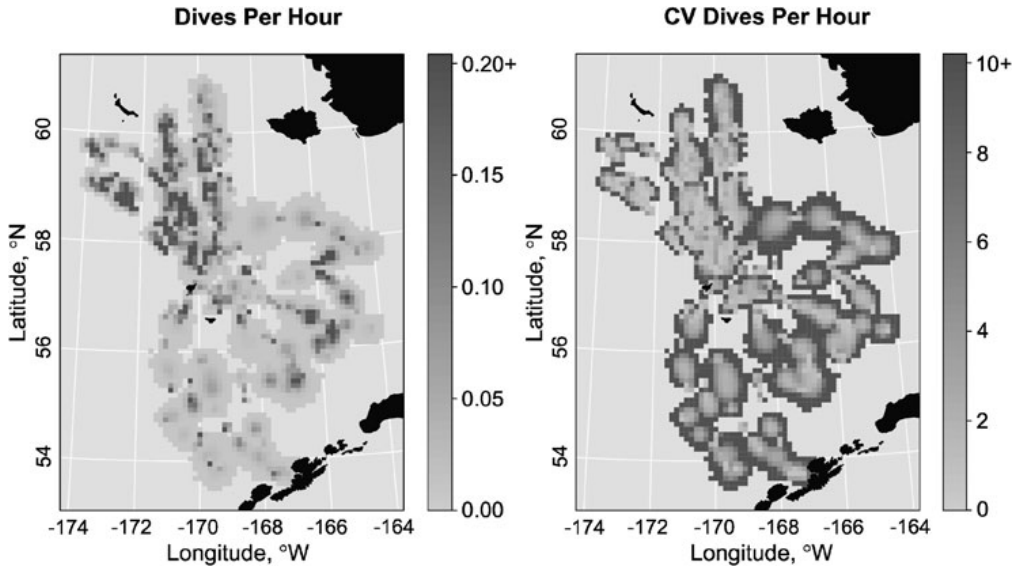

Figure 4. Diving intensity of female northern fur seals in the Pribilof Is., Alaska. The left-hand plot shows the posterior mean number of dives per hour. The right-hand plot shows the posterior coefficient of variation for the posterior distribution of spatial foraging intensity.

Figure 4 illustrates the spatial diving intensity of these animals. The first plot shows the posterior mean diving intensity over the eastern Bering Sea. In general, more foraging dives can be seen north of the Pribilof Islands. The second plot shows the CV of diving intensity. As expected, there is increasing uncertainty near the spatial boundary of estimated foraging intensity. Animals who forage in the region to the north tend to use space along the entire trip for diving, whereas animals to the south and east tend to forage more in hot spots. Further investigation is needed to determine if this might be a function of behavioral differences or prey availability in these regions.

4. DISCUSSION

In this paper we presented an alternative to traditional methods of space use inference as well as other movement metrics. Instead of considering telemetry locations to be independent realizations of a point process, we took a data augmentation approach which considers metrics to be the summarization of the complete, but unknown, path of the animal. The augmentation method uses complex movement modeling to incorporate location uncertainty making it possible to estimate space use for events that have no associated observed location or calculate or any other metric which is affected by location uncertainty.

Along with a path simulation algorithm we presented three methods to deal with propagation of parameter uncertainty to metric inference. The first (and simplest) is to use the posterior mode and assume that parameter uncertainty is negligible compared to location uncertainty. For some studies this may be sufficient, e.g., possibly those using GPS telemetry devices that have trivial observation error. Method 2 uses the SIR algorithm and stochastic integration. Finally, method 3 uses an adaptive deterministic INLA algorithm.

Both methods 2 and 3 have benefits and drawbacks. First the SIR method is based on stochastic integration which is slow to converge; $\mathcal{O}(N^{-1/2})$, where N here is the size of the initial SIR sample. Quadrature methods, such as the INLA method, offer convergence of $\mathcal{O}(N^{-2})$ or better (Givens and Hoeting 2005, p. 144). Quadrature methods, however, fall quickly to the "curse of dimensionality" and become numerically cumbersome as the number of parameters increases past 6. For example, with the INLA method ($\delta_z = 1$ and $\delta_\pi = 2.5$), if we had one additional parameter in our analysis we would have to evaluate 15,625 grid points under posterior normality. The SIR method, however, may also need a large sample due to its slow convergence in a high dimensional situation. Even though the INLA method may require a large number of posterior evaluations, its adaptive deterministic nature makes it a less volatile approximation. The SIR method is critically dependent on the distribution used for the initial sampler. If the tails of the initial sampler are too light, $\boldsymbol{\theta}$ values away from the mode will tend to have the highest weights or be dominated by a single $\boldsymbol{\theta}$ value. This often requires some level of researcher interaction with the simulation in each animal to assure this does not cause serious errors. The INLA method is robust to this problem at the expense of under representing the parameter uncertainty (grid too coarse) or excessive posterior evaluations (grid too fine). Because it is using a grid, however, the sample points will have the same relative weight as the posterior. Thus the mode always has the highest weight with the INLA method.

In our example analysis the number of posterior evaluations with the INLA method never exceeded the expected number under posterior normality. No doubt, some of this effect was due to the fact that the posterior is truncated with respect to the location error parameters. This suggests that the posterior is not especially heavy-tailed. Thus, the SIR method turned out to be fairly efficient, resulting, on average, in an effective sample size of about one half the number of actual draws. Because our example contained a small number of animals, the efficiency probably could have been improved by hand-tuning for each animal by investigating different distributions. This is what we would suggest for small studies. If the number of animals is large (hundreds), however, this becomes impractical and we suggest using the INLA method (provided $\dim(\boldsymbol{\theta}) \leq 5$). It provides some level of parameter uncertainty propagation without intense researcher supervision.

There are certainly many extensions or improvements that can be made to the $\boldsymbol{\theta}$ sample methods we have presented herein. We provided a very basic implementation of the SIR algorithm. There is a wealth of literature concerned with improving importance sampling proposals as well as improved quadrature methods. Durbin and Koopman (2001, p. 208) present an importance sampling method for when $\boldsymbol{\varepsilon}_i$ and $\boldsymbol{\eta}_i$ are t-distributed for heavy-tailed movement and error. Our goal is to present a general framework for estimating movement metrics. Even using the posterior-mode-only method eliminates the pitfalls of the kernel method of space use inference and allows incorporation of complex movement models, autocorrelation, and location uncertainty. In addition, the presented method is compatible with increasing telemetry device capability. As technology increases, telemetry devices will come ever closer to reconstructing the entire path of an animal, as well as recording other variables concerning environment and movement. This method is compatible with that eventual technological goal.

[Accepted December 2010. Published Online February 2011.]

REFERENCES

Anderson-Sprecher, R., and Ledolter, J. (1991), "State-space Analysis of Wildlife Telemetry Data," *Journal of the American Statistical Association*, 86, 596–602.

Blundell, G. M., Maier, J. A. K., and Debevec, E. M. (2001), "Linear Home Ranges: Effects of Smoothing, Sample Size, and Autocorrelation on Kernel Estimates," *Ecological Monographs*, 71, 469–489.

CLS (2008), "Argos user's manual," *http://www.argos-system.org/manual/*.

de Jong, P., and Penzer, J. (1998), "Diagnosing Shocks in Time Series," *Journal of the American Statistical Association*, 93, 796–806.

Durbin, J., and Koopman, S. (2001), *Time Series Analysis by State Space Methods*, Oxford: Oxford University Press. 253 pp.

——— (2002), "A Simple and Efficient Simulation Smoother for State Space Time Series Analysis," *Biometrika*, 89, 603–615.

Fieberg, J. (2007a), "Kernel Density Estimators of Home Range: Smoothing and the Autocorrelation Red Herring," *Ecology*, 88, 1059–1066.

——— (2007b), "Utilization Distribution Estimation Using Weighted Kernel Density Estimators," *Journal of Wildlife Management*, 71, 1669–1675.

Givens, G., and Hoeting, J. A. (2005), *Computational Statistics*, New York: Wiley.

Goebel, M. E. (1998), "Female Foraging Behavior: Inter- and Intra-annual Variation in Individuals," in *Behavior and Ecology of the Northern Fur Seal*, ed. R. Gentry, Princeton: Princeton University Press, pp. 243–259.

Gurarie, E., Andrews, R., and Laidre, K. (2009), "A Novel Method for Identifying Behavioural Changes in Animal Movement Data," *Ecology Letters*, 12, 395–408.

Horne, J., and Garton, E. (2006), "Selecting the Best Home Range Model: An Information-Theoretic Approach," *Ecology*, 87, 1146–1152.

Horne, J. S., Garton, E. O., Krone, S. M., and Lewis, J. S. (2007), "Analyzing Animal Movements Using Brownian Bridges," *Ecology*, 88, 2354–2363.

Johnson, D. S., London, J. M., Lea, M.-A., and Durban, J. W. (2008), "Continuous-time Correlated Random Walk Model for Animal Telemetry Data," *Ecology*, 89, 1208–1215.

Jonsen, I., Flemming, J., and Myers, R. (2005), "Robust State-space Modeling of Animal Movement Data," *Ecology*, 86, 2874–2880.

Jonsen, I. D., Myers, R. A., and Flemming, J. M. (2003), "Meta-analysis of Animal Movement Using State-space Models," *Ecology*, 84, 3005–3063.

Jonsen, I. D., Myers, R. A., and James, M. C. (2007), "Identifying Leatherback Turtle Foraging Behaviour from Satellite Telemetry Using a Switching State-space Model," *Marine Ecology-Progress Series*, 337, 255–264.

Katajisto, J., and Moilanen, A. (2006), "Kernel-based Home Range Method for Data With Irregular Sampling Intervals," *Ecological Modelling*, 194, 405–413.

Kuhn, C. E., Crocker, D. E., Tremblay, Y., and Costa, D. P. (2009a), "Time to Eat: Measurements of Feeding Behaviour in a Large Marine Predator, the Northern Elephant Seal *Mirounga Angustirostris*," *Journal of Animal Ecology*, 78, 513–523.

Kuhn, C. E., Johnson, D. S., Ream, R. R., and Gelatt, T. S. (2009b), "Advances in the Tracking of Marine Species: Using GPS Locations to Evaluate Satellite Track Data and a Continuous-time Movement Model," *Marine Ecology Progress Series*, 393, 97–109.

Morales, J. M., Haydon, D. T., Friar, J., Holsinger, K. E., and Fryxell, J. M. (2004), "Extracting More out of Location Data: Building Movement Models as Mixtures of Random Walks," *Ecology*, 85, 2436–2445.

Otis, D. L., and White, G. C. (1999), "Autocorrelation of Location Estimates and the Analysis of Radiotracking Data," *Journal of Wildlife Management*, 63, 1039–1044.

Patterson, T. A., Thomas, L., Wilcox, C., Ovaskainen, O., and Matthiopoulis, J. (2008), "State-space Models of Individual Animal Movement," *Trends in Ecology and Evolution*, 23, 87–94.

R Development Core Team (2010), *R: A Language and Environment for Statistical Computing*, Vienna: R Foundation for Statistical Computing. *http://www.R-project.org*. ISBN 3-900051-07-0.

Rue, H., Martino, S., and Chopin, N. (2009), "Approximate Bayesian Inference for Latent Gaussian Models by Using Integrated Nested Laplace Approximations," *Journal of the Royal Statistical Society, Series B—Statistical Methodology*, 71, 319–392.

Van Winkle, W. (1975), "Comparison of Several Probabilistic Home-range Models," *Journal of Wildlife Management*, 39, 118–123.

Worton, B. J. (1989), "Kernel Methods for Estimating the Utilization Distribution in Home-range Studies," *Ecology*, 70, 164–168.